CHAPTER - 8.

STUDIES OF PHOTOELECTROCHEMICAL SOLAR CELLS FABRICATED USING AS-GROWN AND CADMIUM DOPED $CuInS_2$ SINGLE CRYSTALS

8.1. INTRODUCTION

The use of transition metal dichalcogenides having MoS_2 type structure, for solar energy conversion in photoelectrochemical cells has been widely accepted due to its small bandgap energy and high chemical stability [1-2]. But the optical energy conversion yield of these layered semiconductors turns out to be lower than theoretically expected from their bandgaps [3]. The main reason for this behaviour is connected with the existence of an indirect bandgap which restricts light absorption in a considerable energy quantum range above the bandgap. One should therefore try to consider materials with direct bandgaps for fabrication of photoelectrochemical solar cells. During the course of investigation on various materials we have found that $CuInS_2$ is a direct bandgap semiconductor with very high value of absorption coefficient. Efforts have therefore been made in this chapter to carry out a photoelectrochemical characterisation of $CuInS_2$ single crystals grown by a chemical vapour transport technique.

We have already seen from the literature survey presented in chapter 1 that $CuInX_2$ (X = S or Se) crystallizing in the chalcopyrite structure is a direct bandgap semiconductor, exhibiting interesting optoelectronic behaviour [4]. The

partial Cu-d character of the top of the valence band in these compounds, which gives less of a bond-breaking character has been noted. Uptil now, $CuInSe_2$ is probably the most studied of the compounds by virtue of very promising photovoltaic activity of thin film solar cells containing this semiconductor as the photovoltaic material. A number of investigators [5-16] have shown that $CuInSe_2$ can be used as photoanode in a polysulfide containing photoelectrochemical cell (PEC). Such cells show respectable photovoltaic activity and very good output stability. n-$CuInS_2$ [17,18] can also be used as a photoanode in a PEC cell with polysulfide electrolyte. Cahen et al. [19-21] have reported that efficient and relatively stable photoelectrochemical solar cells can be made using $CuInX_2$ as the photoanodes in contact with aqueous polysulfide electrolytes.

Since as-grown crystals of $CuInS_2$ are semi-insulating, n-type, with 10^5-10^6 ohm.cm. resistivity, it will be difficult to observe any photoelectrochemical activity with them. Hence to obtain material with reasonable resistivity, the as-grown crystals of $CuInS_2$ were doped with cadmium as described in chapter 5.

In the first half of this chapter an evaluation of

the flat band potential using Mott-Schottky plots (Chapter 7) and location of the valence and conduction band will be undertaken. From a knowledge of the redox potential of the electrolyte, the suitability of the electrolyte will be decided.

Using the electrolyte decided above for $CuInS_2$ crystals, an effort will be made in the remaining half of the chapter to see the effect of doping on the photoelectrochemical response of the cadmium doped $CuInS_2$ single crystals.

8.2. EXPERIMENTAL

8.2.1. Crystal Growth And Doping

Single crystals of $CuInS_2$ were grown successfully employing CVT technique using iodine as the transporting agent. Complete growth details are given in chapter 3. Since the as-grown crystals were highly resistive and did not exhibit any photoresponse with PEC cells, they were doped with suitable cadmium dopant to decrease the resistivity. The details of the doping experiments are given in chapter 5.

Different doping concentrations employed for doping the $CuInS_2$ crystals are detailed in **Table 8.1.**

Photoelectrochemical solar cells were first fabricated using the as-grown (CVT) crystals of $CuInS_2$ photoelectrodes in polysulfide electrolytes. Of the different concentration of polysulfide electrolytes used, the best suitable electrolyte was determined using the Mott-Schottky plots.

Using the most suitable polysulfide electrolyte, PEC cells were fabricated using the cadmium doped samples S1, S2 and S3 as photoelectrodes. Complete photoresponse studies were carried out for these PEC cells. Short circuit current (I_{sc}), open circuit voltage (V_{oc}), efficiency (η) etc. were determined and from results thus obtained, the effect of cadmium doping on the cell performance was evaluated.

8.2.2. Electrode And Electrolyte Preparation

A glass rod with a narrow bore was used to prepare the electrode. One end of the narrow bore glass tube was flattened by hot blow. The flat portion was used as a platform for resting the semiconductor crystal. The narrow bore was used as a passage for traversing a good conducting copper wire. The copper wire was flattened at one end for getting good contact with the crystal. An electrical contact was

finally devised with an adhesive silver paste and the copper wire on the back side of the crystal surface. Then the back side of the semiconductor was covered with an adhesive epoxy resin (araldite) leaving a light exposed area. The so prepared complete device of the electrode is shown in Fig. 8.1.

Different concentrations of polysulfide electrolyte were prepared by mixing proper quantity of reagent grade Na_2S, NaOH and S in double distilled water.

8.2.3. Solar Cell Fabrication

The semiconductor electrode prepared in the manner outlined above was immersed in a polysulfide electrolyte contained in a corning glass beaker. A platinum grid (3 cm x 3 cm) was used as the counter electrode. A schematic diagram showing the PEC solar cell is given in Fig. 8.2.

PEC cells prepared with as-grown $CuInS_2$/ polysulfide electrolyte were characterised by Mott-Schottky plots to determine the most suitable electrolyte.

This electrolyte was then used with the PEC solar cells prepared from doped $CuInS_2$ crystals as photoelectrodes. Detailed studies on effect of doping concentration on photo-

electrochemical response were then carried out on these cells.

8.2.4. Mott-Schottky Plots

Mott-Schottky plots were obtained by measuring the capacitance across the as-grown $CuInS_2$ / polysulfide PEC cell at different d.c. bias voltages for all the electrolytes. The capacitance of solid /liquid interface in the PEC solar cells varies from a few μf to pf. It becomes highly difficult to measure the values accurately using normal laboratory LCR meter. To measure the space charge capacitance in the above mentioned range, the Hewlett-Packard model 14274-A multi-frequency LCR meter was therefore deployed. It is a fully tested instrument to measure various electrical component parameter values with substantial accuracy at desired frequency. It can also measure the inductance, susceptance, reactance and in addition, absolute value of vector impedance and phase angle over a wide range with speed. It can be operated in a frequency range of 100 Hz-100KHz. The schematic diagram for impedance measurements is demonstrated in Fig. 8.3. A saturated calomel electrode (SCE) was used as a reference electrode and platinum grid as a counter electrode.

From the Mott-Schottky plots of the above discussed $CuInS_2$ / polysulfide PEC cells, most suitable electrolyte for

optimum PEC performance was determined.

8.2.5. Photoresponse Studies Of Cd Doped PEC Cells

The suitable electrolyte for best performance of as-grown $CuInS_2$ / polysulfide PEC cells obtained from the Mott-Schottky evaluations was used for fabrication of PEC cells with photoelectrodes prepared from Cd doped samples S1, S2 and S3. Current-voltage measurements were carried out at different intensities of incident light. Light source used to obtain photoresponse was a tungsten halogen incandescent lamp. For varying the intensity of light the distance between the source and photoelectrode was varied. The intensity of illumination was measured using "Suryamapi", the light intensity measuring instrument developed by Central Electronics Limited (CEL), India. Generated photovoltages and photocurrents were measured using digital multimeters with the circuit setup as shown in Fig. 8.2.

The maximum output power was obtained from the I-V characteristics, while input power was measured using Suryamapi. For calculating the efficiency (η) and fill factor (FF) of the cell, following equations were used

$$\text{Efficiency } \eta = \frac{\text{Maximum output power x 100 \%}}{\text{Input Power x Area}}$$

$$\text{Fill Factor F.F.} = \frac{I_{mp} \cdot V_{mp}}{I_{sc} \cdot V_{oc}}$$

where I_{mp} and V_{mp} are the photocurrent and photovoltage at maximum power.

I_{sc} and V_{oc} are the short circuit current and open circuit voltage after illumination.

8.3. RESULTS AND DISCUSSION

8.3.1. Mott-Schottky Evaluation

According to the depletion layer approximation the capacitance of the space charge layer varies with the potential drop across the surface according to the Mott-Schottky [23] relation

$$\frac{1}{C^2} = \frac{2}{\epsilon \epsilon_o e N_D} \left[|U_{sce}| - \frac{kT}{e} \right]$$

where ϵ is the dielectric constant, ϵ_o the

permittivity of free space, e the charge of the electron, N_D the donor concentration, U_{SCE} the applied potential drop across the space charge layer, which can be expressed by

$$U_{SCE} = U - U_{FB}$$

U_{FB} is the flat band potential. Mott-Schottky plots of as-grown $CuInS_2$ electrodes with different concentrations of polysulfide electrolytes are depicted in Fig. 8.4 (a and b).The nature of the plots firmly confirms the n-type conducting nature of the single crystals of $CuInS_2$ used in the present study. This also supports the conjecture already made in Chapter 4 about their semiconducting nature by hot probe technique. The donor concentration N_D were determined from the slope of Mott-Schottky relation as

$$N_D = 2 \left[e \epsilon\epsilon_o \, (\text{slope})^{-1} \right]$$

Where ϵ is the dielectric constant of the crystal. For $CuInS_2$, the dielectric constant $\epsilon = 11$ [24]. The donor concentration calculated using the above relations is shown in **Table 8.2.**

The distance between conduction band minimum E_C, and flatband potential U_{FB} is important to localise the

valence band maximum.

According to Kautek et al. [25], in the classical approximation where $(E_C - E_{FB}) / kT > 1$, the effective density of conduction states is given by [26],

$$N_C = \frac{2}{h^3} (2\pi m_e^* kT)^{3/2}$$

where m_e^* is effective mass of electron and is taken to be 0.16 m_e, [24], m_e is the electron mass, N_C comes out to be 1.6×10^{18} cm^{-3}. Assuming that all donors are ionized and have given their electrons into the conduction band, we get the classical Maxwell-Boltzmann distribution.

$$E_C - E_{FB} = kT \ln N_C/N_D$$

$$E - E_{FB} = - e(U - U_{FB})$$

Using the above equation we obtained the difference between fermi level and the edge of the conduction band, $E_C - E_F$, for $CuInS_2$. By subtracting the bandgap energy from the values of E_c, the conduction band, and the valence band positions were located as depicted in Fig. 8.5.

The value of the flat band potential, U_{FB}, of an n-type or p-type semiconductor can be used to predetermine the maximum open circuit photovoltage, $V_{OC(max)}$ of a given semiconductor /electrolyte/ counter electrode cell according to the relation [27],

$$V_{OC(max)} = U_{(redox)} - U_{FB}$$

where $U_{(redox)}$ is the redox potential of the electrolyte. Calculation of V_{oc} using the above relation, shows that electrolyte (d) provides the maximum open circuit voltage $V_{OC(max)}$, thereby suggesting its suitability for PEC solar cells fabricated with $CuInS_2$ single crystals.

8.3.2. Photoresponse Studies Of PEC Cells

The above determined most suitable electrolyte for $CuInS_2$ PEC solar cell from **Table 8.1** i.e. 3M Na_2S + 3M NaOH + 3 M S was used in the subsequent photoresponse experimental work of PEC with cadmium doped $CuInS_2$ samples S1, S2 and S3 as photoelectrodes.

Photoresponse of electrode surface is very important in studying the behaviour of PEC cells. When photon strikes a semiconductor electrode, minority charge carriers are generated in it which move towards the semiconductor /

electrolyte interface. They then pass through the interface into the electrolyte and chemical reaction occurs. If former action is rate determining then there is no role of electrolyte and a PEC cell behaves as p-n junction (Solid State junction) cell. On the other hand if latter action is rate determining, then behaviour is much more complex. Hence to understand which action is dominant the study of electrodes photoresponse is very essential. In order to study this photoresponse, variation of photocurrent-photovoltage characteristic, short circuit current (I_{sc}), open circuit voltage (V_{oc}), fill factor (FF) and efficiency (η), with incident light intensity have been determined. From this photoresponse variation of different PEC parameters, the effect of cadmium concentration on its optimum performance was determined as below.

Fig. 8.6 (a, b & c) gives the photo J-V characteristic plots for the readings tabulated in **Table 8.3** of the PEC solar cells for samples S1, S2 and S3 respectively. It shows that the maximum photocurrent and photovoltage are obtained for sample S3. From which it was inferred that photoresponse is maximum in the lightly doped sample of $CuInS_2$ i.e. S3.

Similarly Fig. 8.7(a, b, & c) shows the plot of shot circuit current (I_{sc})/ open circuit voltage (V_{oc}) versus incident light intensity for the samples S1, S2 and S3 respectively. It is observed that in all cases I_{sc} and V_{oc} shows linear behaviour with light intensity upto 100 mW/cm^2. This linear behaviour shows that the carrier generation is the rate determining action. This variation of V_{oc} and I_{sc} values for each intensity clearly shows that maximum value is obtained for sample S3. This further enhances the above confirmation that PEC photoresponse behaviour is best for lightly doped sample S3.

Figure 8.8 (a, b & c) shows the variation of FF and η values with light intensity for samples S1, S2 & S3 respectively. As seen from these plots, FF and efficiency (η) values show linear decrease with intensities upto 100 mW/cm^2, except in case of FF for sample S3. In sample S3, FF shows an initial decrease upto 40 mW/cm^2 followed by a linear increase thereafter.

From these above plots, it is seen that maximum efficiency (η) values are obtained for sample S3 at all intensities compared to other doped samples. Thus highest PEC response is obtained in sample S3, confirming once again the

earlier result that best performance is obtained with the lightly doped cadmium $CuInS_2$ samples.

8.4. CONCLUSIONS

1. From the Mott-Schottky plots of as-grown $CuInS_2$/ polysulfide electrolyte PEC cell, electrolyte (d) i.e. 3M Na_2S + 3M NaOH + 3M S provides the maximum theoretical open circuit voltage.
2. The proximity of the redox level to the valence band edge (Fig. 8.5) in this (d) electrolyte, suggests that charge transfer is more likely to occur via valence band.
3. Location of the redox level nearer to valence band (Fig. 8.5) further suggests that this (d) electrolyte will be appropriate for PEC cells fabricated with $CuInS_2$ [28].
4. Photoresponse of cadmium doped $CuInS_2$ /polysulfide PEC cells for all samples i.e. S1, S2 and S3 shows that the short circuit current (I_{sc}) and open circuit voltage (V_{oc}) increases with increasing intensity adhering to the theoretical expectation discussed above.
5. Maximum efficiency has been found at 20 mW/cm^2 intensity with a linear decrease to a minimum value at

100 mW/cm^2 intensity for all samples S1, S2 & S3.

6. The best photoresponse performance in doped $CuInS_2$/ polysulfide PEC cells has been found with sample S3 i.e. $CuInS_2$ having the lowest concentration of cadmium doping.

7. This above point can be explained on the basis of Rouxel et al. [29] suggestion, that in certain cases the electrons given by the dopant may be trapped in certain sites rather than being delocalised in the conduction band of the host crystal. It was proposed that in such cases the doped atoms might be regarded as analogous to deep level impurities, leading thereby to additional energy level near the top of the valence band or alternatively it may be regarded as a modification of the energy band of the host crystal due to the doping. This may be the probable reason for lower values of PEC solar cell performance in case of heavily doped S1 and S2 samples compared to lightly doped sample S3.

TABLE 8.1 Annelding Concentrations

Sample Nos.	Cadmium Concentrtion mg./c.c.
S1	1.00
S2	0.50
S3	0.25

TABLE 8.2 Different Polysulfide Electrolytes Used And Corresponding Dohnor Concentrations N_D

Electrolyte	N_D cm^{-3}
(a) 1 M Na_2S, 1 M NaOH, 1 MS	6.41×10^{16}
(b) 2 M Na_2S, 2 M NaOH, 2 MS	4.89×10^{16}
(c) 1.5 M Na_2S, 2 M NaOH, 2.5 MS	3.21×10^{16}
(d) 3 M Na_2S, 3 M NaOH, 3 MS	4.93×10^{16}
(e) 1 M Na_2S, 1 M NaOH, 0.1 MS	1.44×10^{17}
(f) 1 M Na_2S, 1 M NaOH, 0.001 MS	1.91×10^{17}

TABLE 8.3(a) J-V Date for Sample S1

20 mW/cm^2		40 mW/cm^2		60 mW/cm^2		80 mW/cm^2		100 mW/cm^2	
V_{oc} = 155.2 mV		V_{oc} = 208.3 mV		V_{oc} = 240.3 mV		V_{oc} = 269 mV		V_{oc} = 280 mV	
I_{sc} = 10.7 uA		I_{sc} = 12.24 uA		I_{sc} = 14.82 uA		I_{sc} = 16.4 uA		I_{sc} = 17.6 uA	
J mA/cm^2	V mV	J mA/cm^2	V mV	J mA/cm^2	V mV	J mA/cm^2	V mV	J mA/cm^2	V mV
0.11	146.7	0.11	189.3	0.11	226.6	0.11	249.7	0.11	258.7
0.22	119.7	0.22	177.2	0.22	195.2	0.22	205.0	0.22	214.7
0.33	106.5	0.33	162.8	0.33	183.9	0.33	196.7	0.33	201.3
0.44	99.8	0.44	153.7	0.44	178.8	0.44	184.4	0.44	196.8
0.55	87.6	0.55	137.6	0.55	163.7	0.55	178.7	0.55	185.7
0.66	77.7	0.66	117.8	0.66	152.0	0.66	169.7	0.66	179.3
0.77	58.8	0.77	92.7	0.77	137.8	0.77	151.8	0.77	168.4
0.88	46.3	0.88	82.9	0.88	118.6	0.88	142.3	0.88	157.6
0.99	23.1	0.99	52.6	0.99	86.7	0.99	124.9	0.99	137.8
1.11	6.6	1.11	28.7	1.11	73.5	1.11	101.6	1.11	102.6
		1.22	8.6	1.22	43.4	1.22	77.6	1.22	89.4
				1.33	22.7	1.33	62.8	1.33	
					5.7	1.44	48.3	1.44	59.4
						1.55	23.7	1.55	37.8
						1.66	6.5	1.66	23.5
								1.77	12.8

TABLE 8.3(b) J-V Data for Sample S2

20 mW/cm^2		40 mW/cm^2		60 mW/cm^2		80 mW/cm^2		100 mW/cm^2	
V_{oc} = 229 mV		V_{oc} = 239 mV		V_{oc} = 275 mV		V_{oc} = 288 mV		V_{oc} = 307 mV	
I_{sc} = 7.0 uA		I_{sc} = 9.1 uA		I_{sc} = 12.2 uA		I_{sc} = 14.6 uA		I_{sc} = 16.01 uA	
J mA/cm^2	V mV	J mA/cm^2	V mV	J mA/cm^2	V mV	J mA/cm^2	V mV	J mA/cm^2	V mV
0.1	200.2	0.1	206.5	0.1	234.7	0.1	244.0	0.1	257.3
0.2	174.5	0.2	183.6	0.2	217.2	0.2	225.0	0.2	240.2
0.3	147.2	0.3	158.2	0.3	196.5	0.3	212.0	0.3	223.2
0.4	118.5	0.4	138.2	0.4	175.4	0.4	192.5	0.4	209.2
0.5	86.6	0.5	120.5	0.5	160.0	0.5	177.0	0.5	191.3
0.6	57.2	0.6	91.0	0.6	135.5	0.6	154.6	0.6	175.8
0.7	9.8	0.7	59.8	0.7	112.0	0.7	125.0	0.7	146.6
		0.8	29.6	0.8	91.0	0.8	114.0	0.8	137.5
		0.9	11.2	0.9	65.0	0.9	89.5	0.9	114.4
				1.0	21.5	1.0	65.2	1.0	93.3
				1.1	10.3	1.1	46.7	1.1	76.5
						1.2	21.4	1.2	57.8
						1.3	17.6	1.3	46.7
						1.4	8.7	1.4	24.6
								1.5	13.3

TABLE 8.3(c) J-V Data For Sample S3

20 mW/cm^2		40 mW/cm^2		60 mW/cm^2		80 mW/cm^2		100 mW/cm^2	
V_{oc} = 241.3 mV		V_{oc} = 265.3 mV		V_{oc} = 305.3 mV		V_{oc} = 320.6 mV		V_{oc} = 334.0 mV	
I_{sc} = 13.8 uA		I_{sc} = 15.3 uA		I_{sc} = 16.8 uA		I_{sc} = 17.9 uA		I_{sc} = 19.4 uA	
J mA/cm^2	V mV	J mA/cm^2	V mV	J mA/cm^2	V mV	J mA/cm^2	V mV	J mA/cm^2	V mV
0.11	235.6	0.11	255.8	0.11	291.7	0.11	312.3	0.11	326.7
0.22	222.1	0.22	247.2	0.22	273.3	0.22	301.3	0.22	319.0
0.33	211.3	0.33	225.3	0.33	257.6	0.33	289.4	0.33	301.7
0.44	193.2	0.44	219.3	0.44	247.0	0.44	277.2	0.44	288.7
0.55	183.3	0.55	201.4	0.55	231.3	0.55	256.7	0.55	272.3
0.66	177.3	0.66	185.0	0.66	211.0	0.66	239.6	0.66	261.8
0.77	150.6	0.77	170.6	0.77	193.7	0.77	225.6	0.77	249.7
0.88	128.7	0.88	151.0	0.88	183.0	0.88	211.8	0.88	235.4
0.99	105.6	0.99	135.3	0.99	165.0	0.99	193.7	0.99	223.7
1.11	92.0	1.11	121.3	1.11	159.8	1.11	181.4	1.11	211.3
1.22	42.0	1.22	82.1	1.22	120.6	1.22	142.2	1.22	183.1
1.33	8.6	1.33	51.0	1.33	91.4	1.33	125.3	1.33	165.4
		1.44	7.8	1.44	63.1	1.44	98.9	1.44	147.3
				1.55	27.3	1.55	57.7	1.55	126.1
				1.66	8.2	1.66	43.1	1.66	119.7
						1.77	6.2	1.77	83.5
								1.88	62.8
								1.99	7.9

CAPTIONS TO THE FIGURES

Fig. 8.1. Schematic diagram of semiconductor electrode used in the PEC set up.

Fig. 8.2. Schematic diagram showing complete PEC solar cell.

Fig. 8.3. Schematic diagram for the impedance (capacitance) measurements.

Fig. 8.4. Mott-Schottky plots (a & b)

Fig. 8.5. Position of band edges of $CuInS_2$ in polysulfide electrolytes, Cb - conduction band edge, vb - valence band edge, E_f-fermi level, U_r - redox level.

Fig. 8.6. (a,b & c) I-V characteristics of PEC solar cells for samples S1, S2 and S3 respectively.

Fig. 8.7. (a, b & c) Plots of I_{sc}/V_{oc} Vs Intensity for samples S1, S2 and S3 respectiveLy.

Fig. 8.8. (a, b & c) Plots of FF/n Vs I_L for samples S1, S2 and S3 respectively.

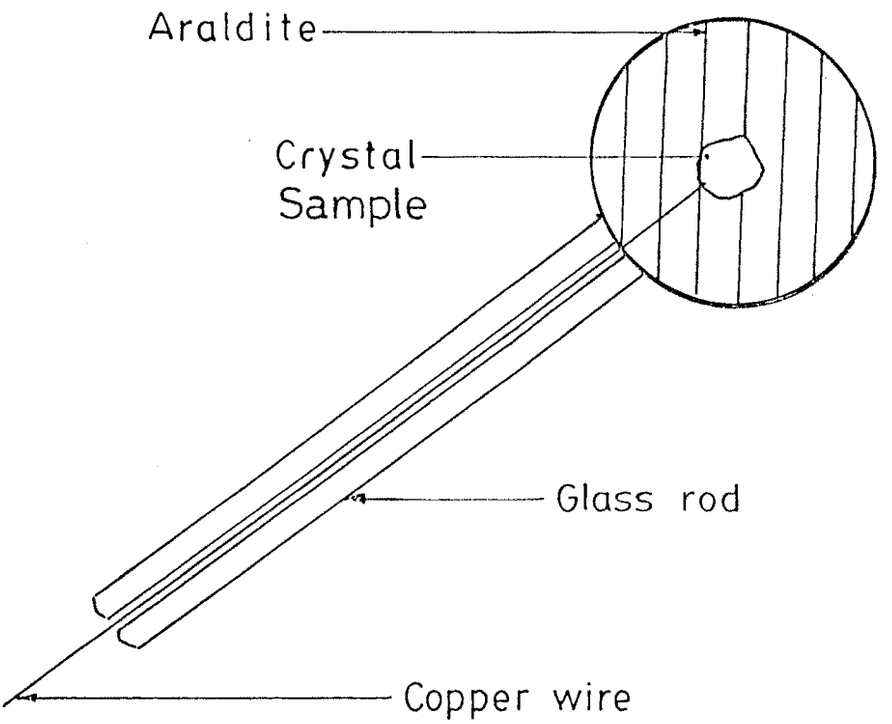

fig 8.1

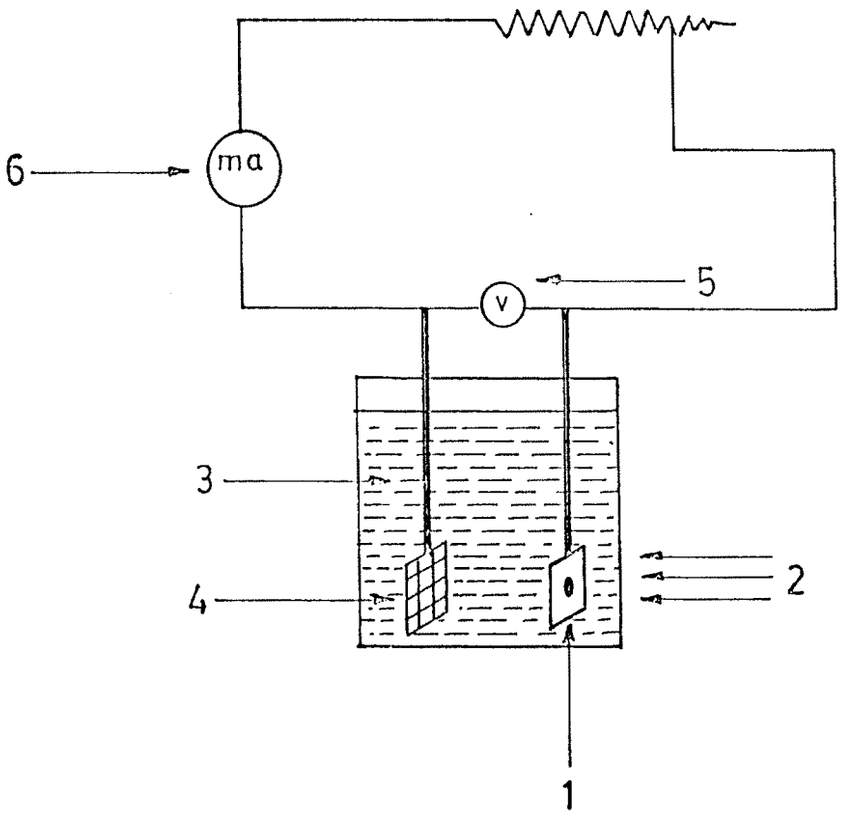

1 Semi conducting crystal.
2 Incident light.
3 Electrolyte
4 Platinum grid
5 Voltmeter
6 Milliammeter

fig. 8·2

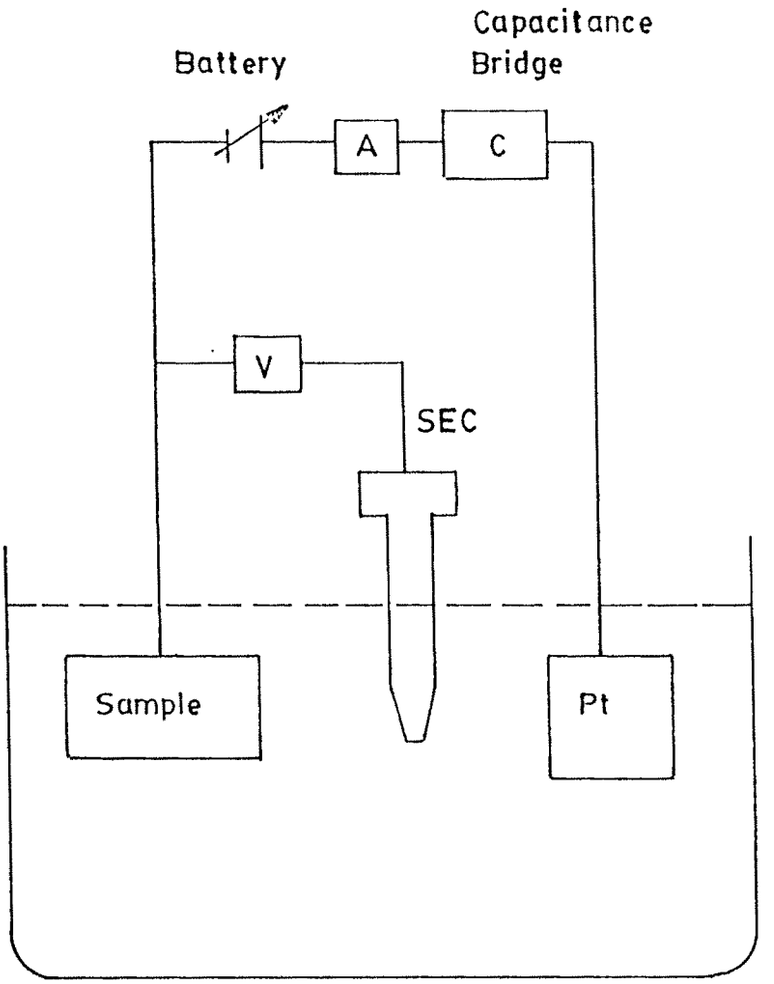

fig. 8·3

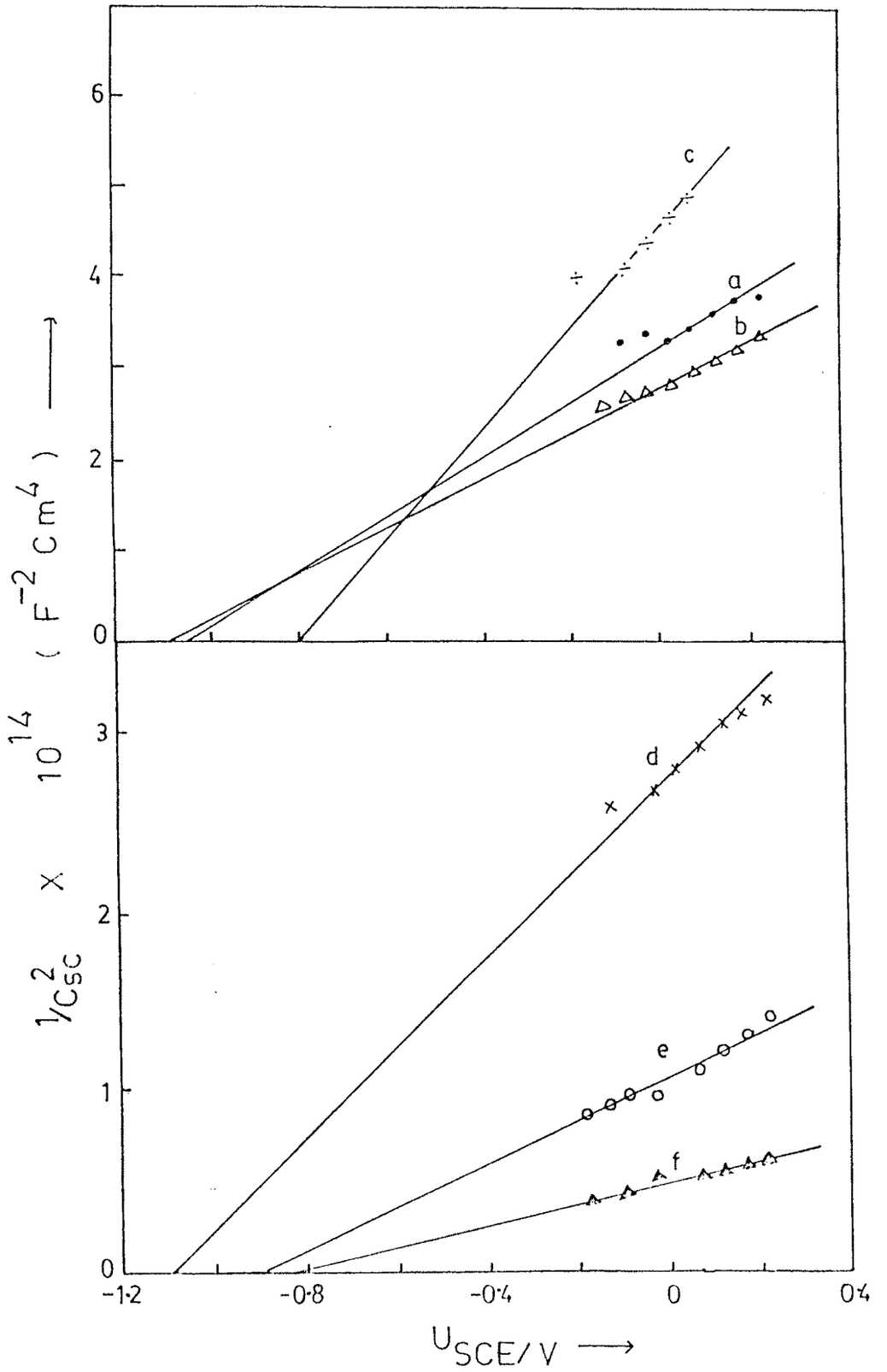

fig 8·4

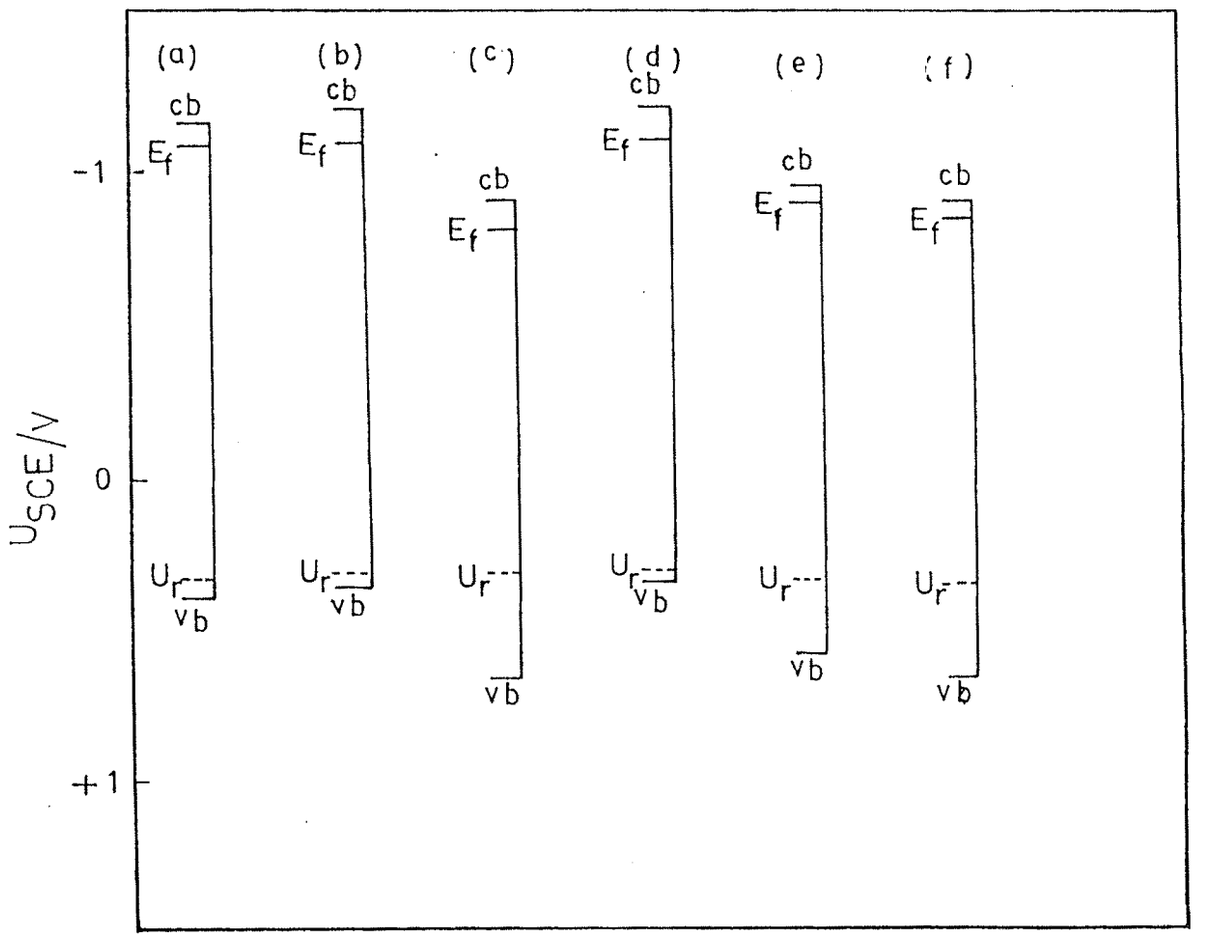

fig 8.5

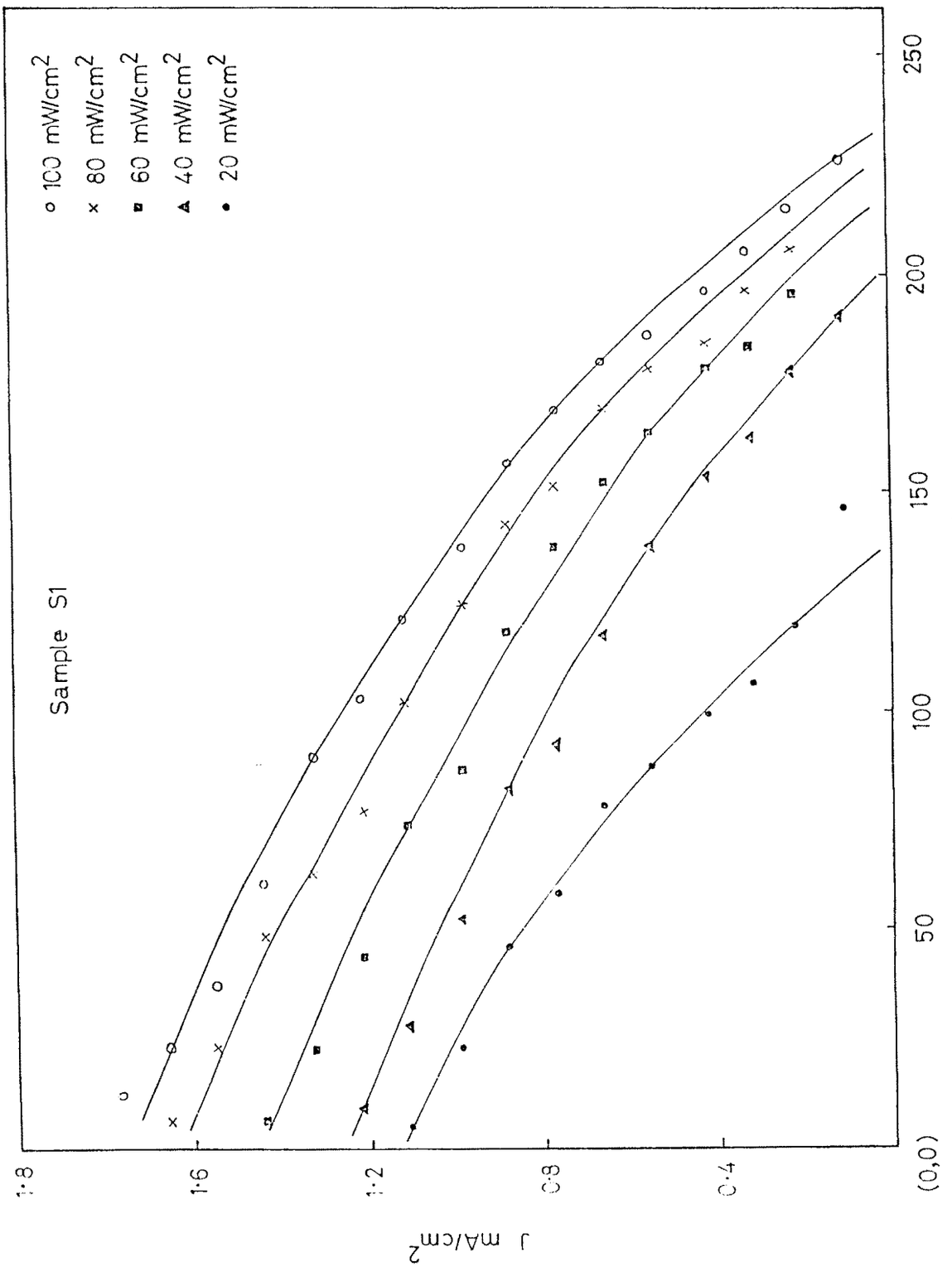
Sample S1
100 mW/cm2
80 mW/cm2
60 mW/cm2
40 mW/cm2
20 mW/cm2
J mA/cm2
1·8
1·6
1·2
0·8
0·4
(0,0)
50
100
150
200
250
Photovoltage (V mV)

fig 8·6(a)

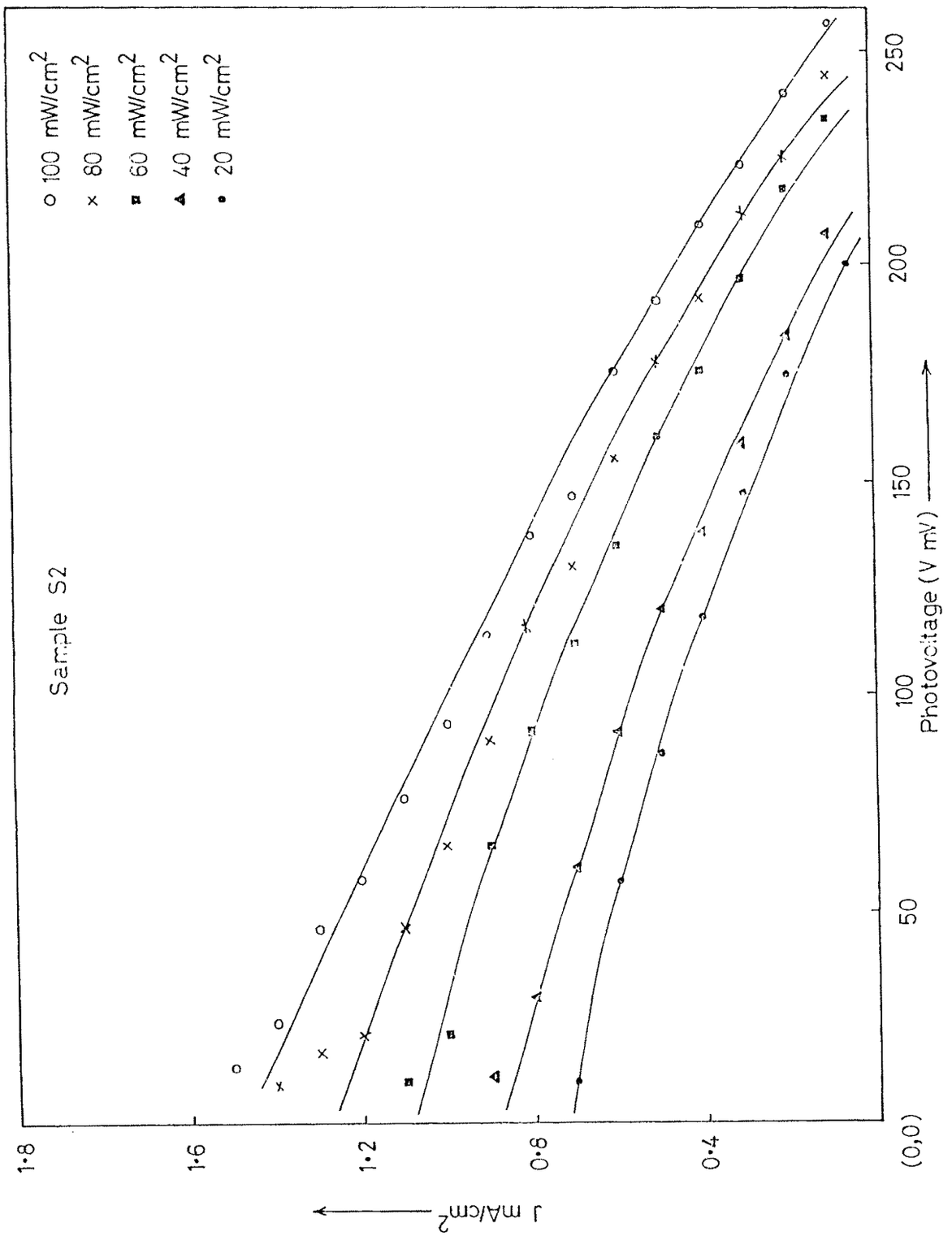
Sample S2
o 100 mW/cm2
× 80 mW/cm2
▪ 60 mW/cm2
▲ 40 mW/cm2
• 20 mW/cm2
J mA/cm2
1·8
1·6
1·2
0·8
0·4
(0,0)
50
100
150
200
250
Photovoltage (V mV)

fig 8·6(b)

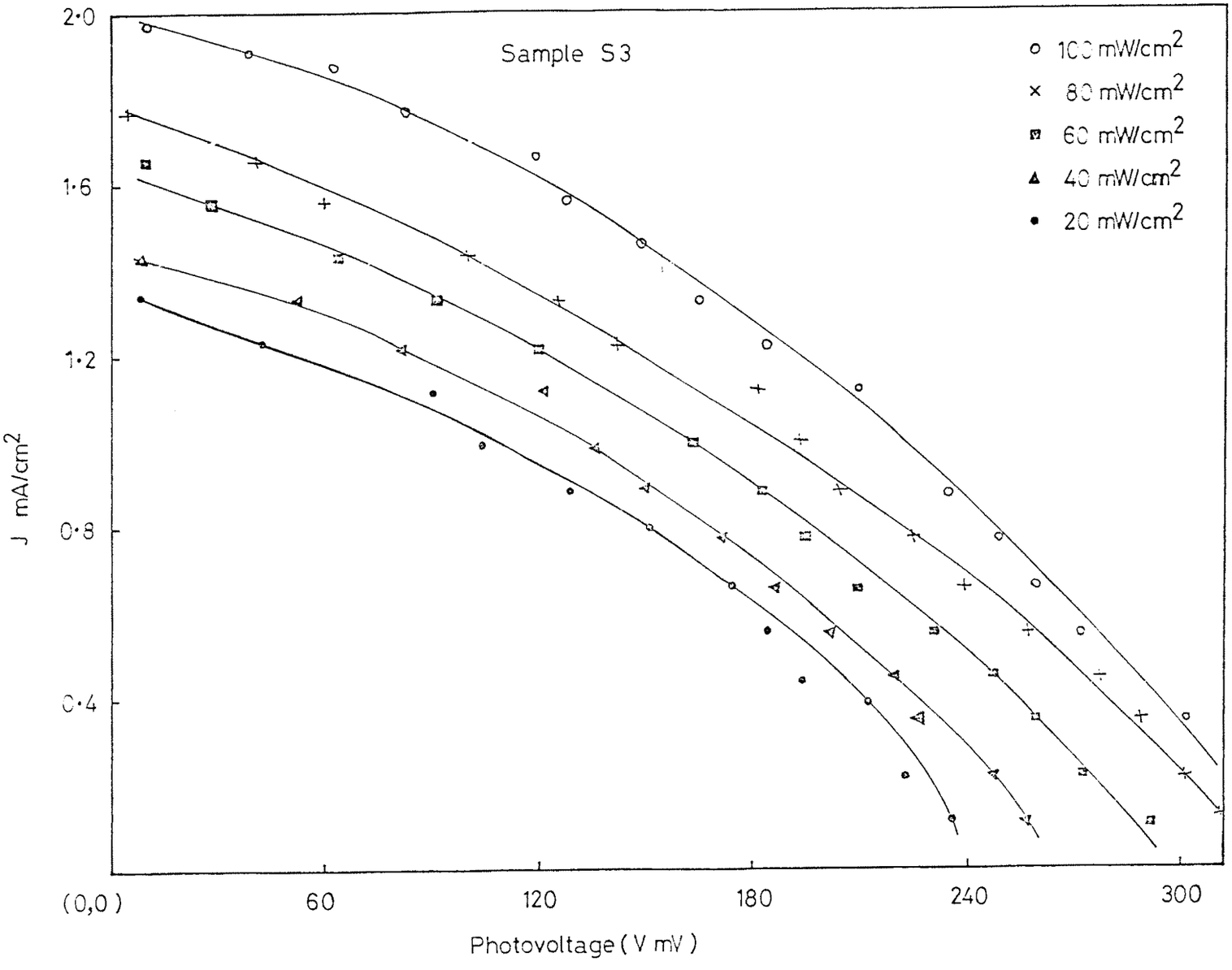
Sample S3
100 mW/cm2
80 mW/cm2
60 mW/cm2
40 mW/cm2
20 mW/cm2
J mA/cm2
2·0
1·6
1·2
0·8
0·4
(0,0)
60
120
180
240
300
Photovoltage (V mV)

fig 8·6 (c)

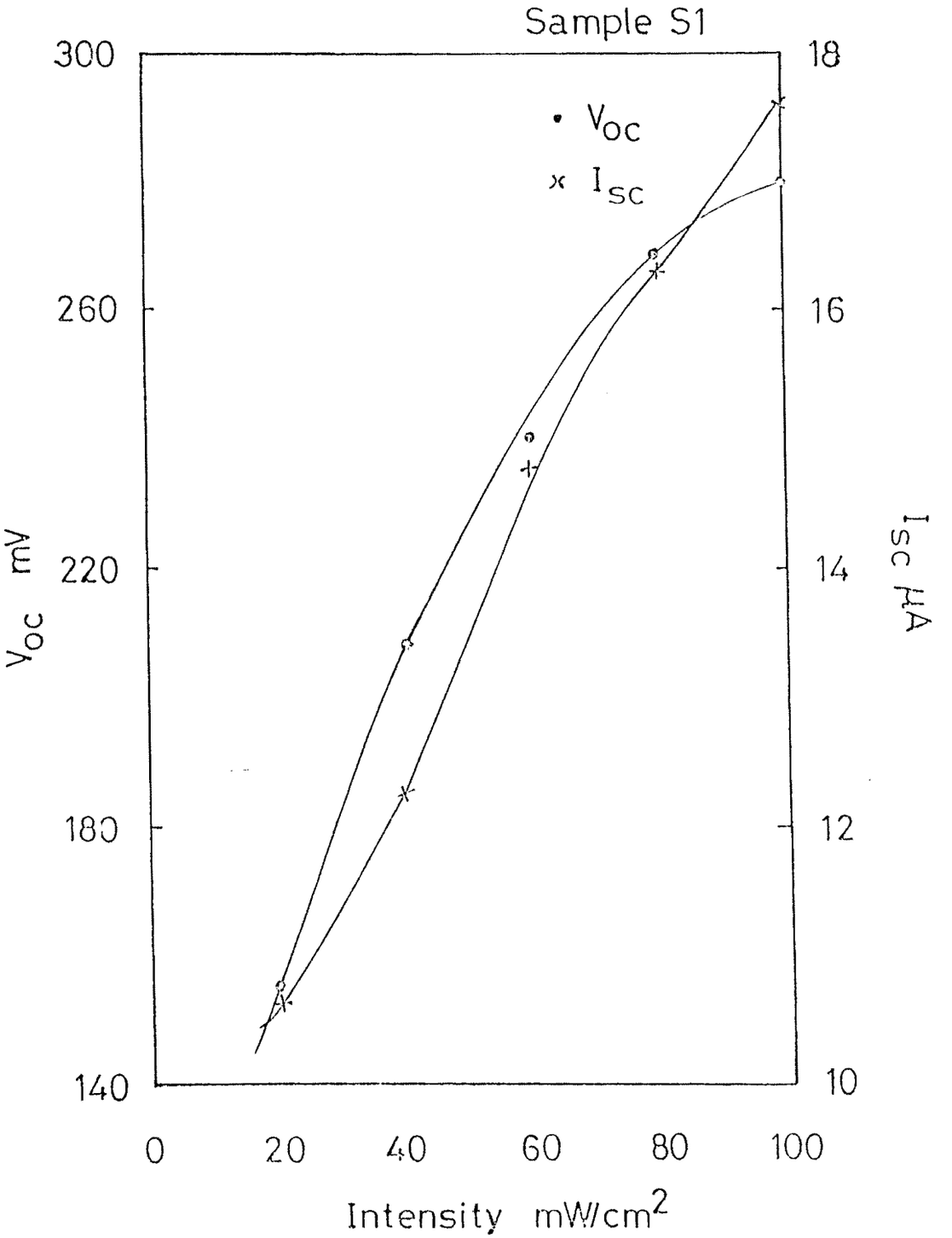
Sample S1
300
260
220
180
140
18
16
14
12
10
• V_{oc}
× I_{sc}
V_{oc} mV
I_{sc} μA
0
20
40
60
80
100
Intensity mW/cm^2

fig 8·7 (a)

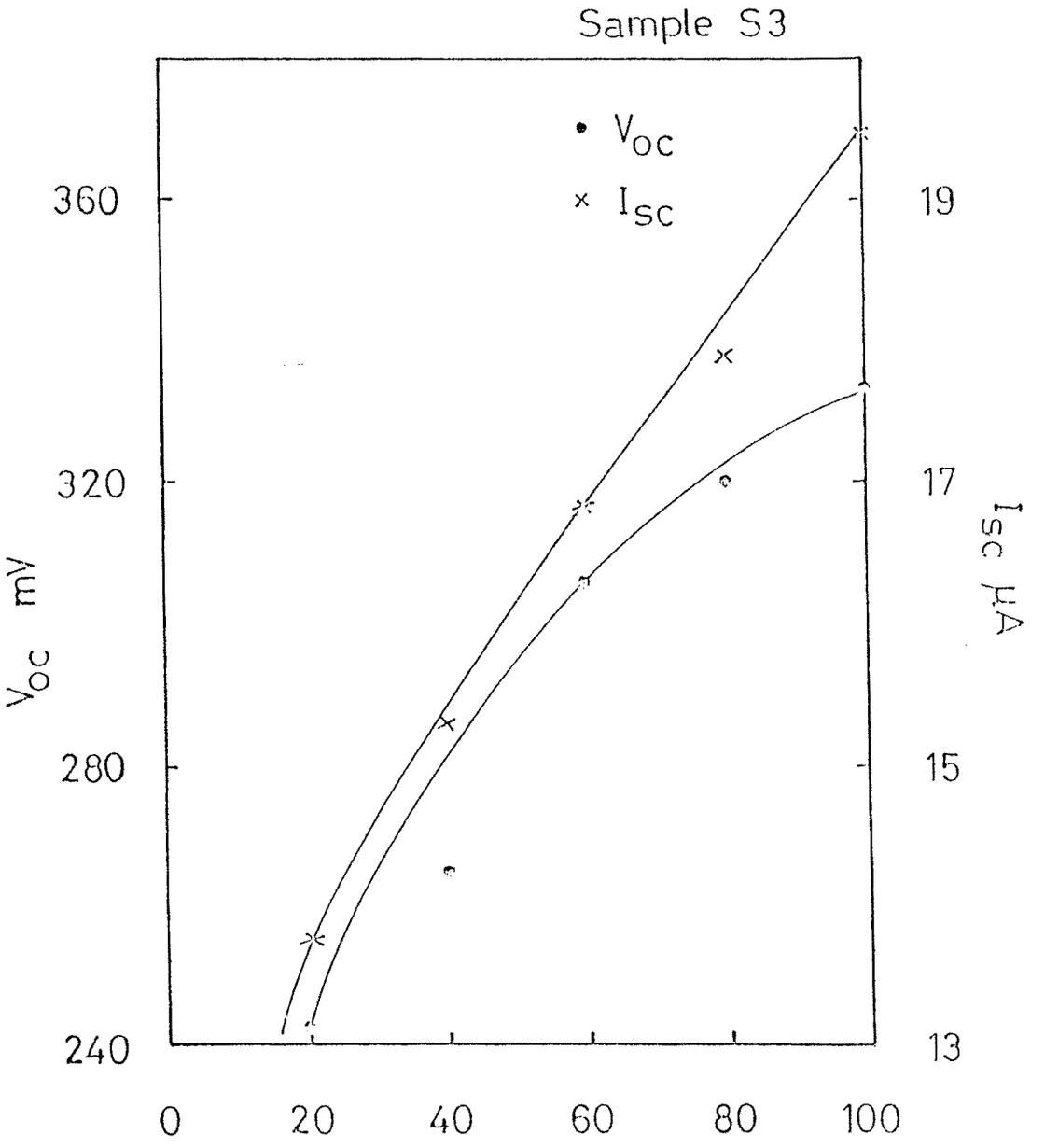
Sample S3
• V_{oc}
× I_{sc}
360
320
280
240
19
17
15
13
V_{oc} mV
I_{sc} μA
0
20
40
60
80
100
Intensity mW/cm^2

fig 8·7(a)

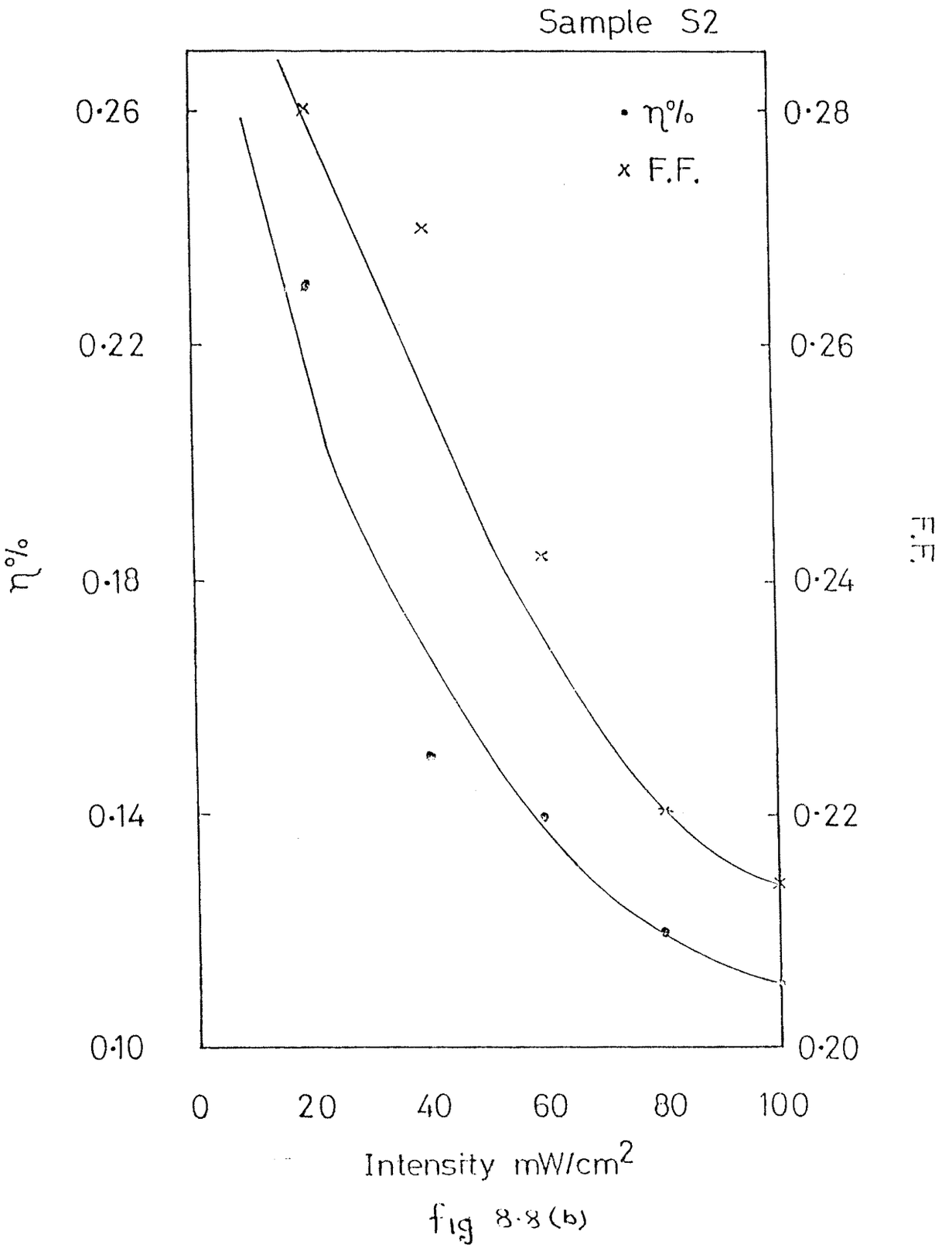
Sample S2
• η%
× F.F.
0·26
0·22
0·18
0·14
0·10
η%
0·28
0·26
0·24
0·22
0·20
F.F.
0
20
40
60
80
100
Intensity mW/cm²

fig 8·8(b)

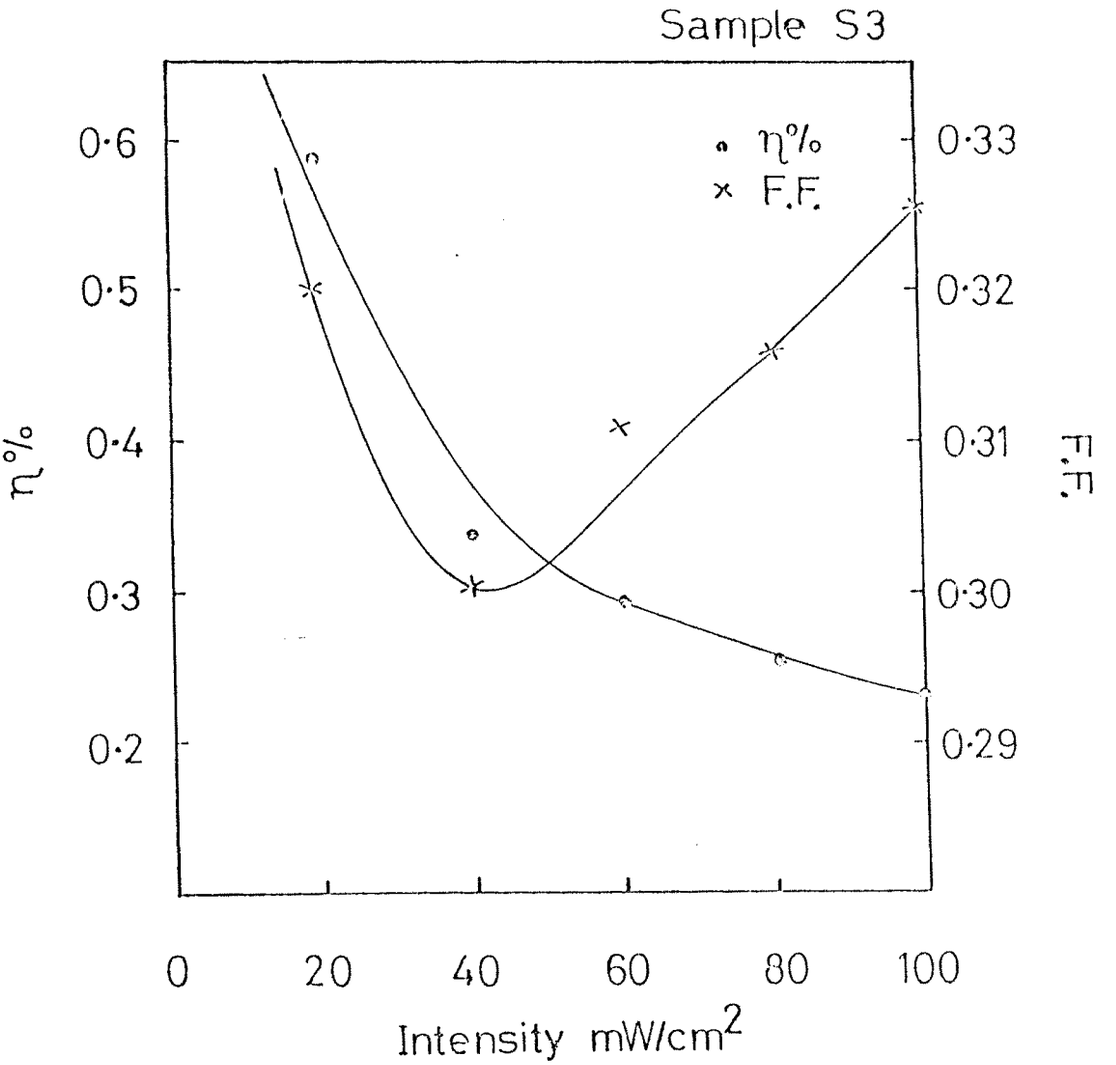
Sample S3
η%
F.F.
0·6
0·5
0·4
0·3
0·2
0·33
0·32
0·31
0·30
0·29
0
20
40
60
80
100
Intensity mW/cm²

fig 8·8 (a)

REFERENCES

1. H. O. Finlelea; "Studies in Physical and Theoretical Chemistry, Semiconductor electrodes" Chap. 10 [Elsevier Sci. Pub., New York] (1988).
2. A. Aruchamy; "Photoelectrochemistry and photovoltatics of Layered Semiconductors" Ed. A. Aruchamy [Kluwer Academic Publ., Boston, U.S.A.] (1992).
3. W. Kautek, J. Grobrecht and H. Gerischer; Ber. Bunsenges, Phys. Chem. **84**, 1034 (1980).
4. J. L. Shay and J. H. Wernick; "Ternary chalcopyrite semiconductor : Growth, Electronic Properties and Applications" [Pergamon Press, Oxford, England] (1975).
5. S. Menezes, H. J. Lewerenz and K. J. Bachmann; Nature **305**, 615 (1983).
6. K. J. Bachmann, S. Menezes, R. Kotz, M. Fearheily and H. J. Lewerenz; Surf. Sci. **138**, 475 (1984).
7. D. Cahen and Y. W. Chen; Appl. Phys. Lett. **45**, 746 (1984).
8. Y. Mirovsky, R. Tenne, D. Cahen, G. Sawatzky and M. Polok; J. Electrochem. Soc. **132**, 1070 (1985).
9. D. Haneman and J. Szot; Appl. Phys. Lett. **46**, 778 (1985).

10. D. Cahen, P. J. Ireland, L. L. Kazmerski and F. A. Thiel; J. Appl. Phys. **57**, 4761 (1985).

11. J. Szot and D. Haneman; J. Appl. Phys. **59**, 2249 (1986).

12. S. Menezes; Solar Cells **16**, 225 (1986).

13. H. J. Lewerenz and E. R. Kotz; J. Appl. Phys. **60**, 1430 (1986).

14. D. Haneman; CRC Crit. Rev. Solid State Mater. Science **14**, 377 (1988).

15. J. W. Chu and D. Haneman; Solar Cells **31**, 197 (1991).

16. G. D. Dagan and D. Cahen; J. Electrochem. Soc. **134**, 592 (1987).

17. M. Robbins, K. J. Bachmann, V. G. Lambrecht, F. A. Thiel, J. Thomson, Jr., B. G. Vadimsky, S. Menezes, A. Heller and B. Miller; J. Electrochem. Soc. **125**, 831 (1978).

18. Y. Mirovsky, D. Cahen, G. Hodes, R. Tenne and W. Giriat; Solar Energy Mater. **4**, 169 (1981).

19. D. Cahen, Y. Mirovsky and R. Tenne; "Solid State Chemistry" Eds. S. R. Metselar, H. J. Heijlegers and J. Schooman [Elsevier, Amsterdam] (1983).

20. Y. M. Mirovsky, G. Djemal and D. Cahen; Nuovo Cimento, **D2**, 2039 (1983).

21. D. Cahen, G. Dagan, G. Hodes, Y. Mirovsky, W. Giriat and M. Luebke; J. Electrochem. Soc. **132**, 1062 (1985).

22. D. Cahen, G. Dagan, G. Hodes, Y. Mirovsky, Y. W. Chen, J. C. W. Folmer, P. J. Ireland, R. Nouti, J. A. Turner, K. J. Bachmann, S. Endo, C. Rincon, G. A. Sawatzky and M. Tankiewicz; Proc. Cryst. Growth Charach. **10**, 263 (1985).

23. (a) W. Schottky; Z. Phys. **113**, 367 (1939).
(b) N. F. Mott; Proc. Roy. Soc. **A 171**. 27 (1939).

24. M. J. Jagadeesh and M. S. Seehra; Sol. State. Commun. **34**, 257 (1980).

25. W. Kautek and H. Gerischer; Ber. Bunsenges. Phys. Chem. **84**, 645 (1980).

26. H. Gerischer; Adv. Electro. Chem. Engg. **1**, 139 (1961).

27. H. Gerischer; J. Electroanal. Chem. Interfacial Electrochem. **58**, 263 (1975).

28. S. G. Patel, S. H. Chaki and A. Agarwal; Bull. of Electrochem. **9**, 32 (1993).

29. J. Rouxel; Mater. Res. Bull. **13**, 1425 (1978).